

Article

# Direct Synthesis of Graphene Quantum Dots with Different Fluorescence Properties by Oxidation of Graphene Oxide Using Nitric Acid

Meilian Zhao

College of Medical Technology, Chengdu University of Traditional Chinese Medicine, Chengdu 611137, China; zhaomeilian2009@126.com; Tel.: +86-286-180-1313

Received: 3 July 2018; Accepted: 2 August 2018; Published: 5 August 2018



**Abstract:** Graphene quantum dots (GQDs) play a critical role in many applications in the electrical and optical fields. We develop a simple three-step hydrothermal etching method to prepare GQDs by adopting graphene oxide (GO) as a precursor and nitric acid as an oxidant. We discuss the formation mechanism of GQDs by the characterization of products and intermediates with Scanning electronic microscopy (SEM), Transmission electron microscopic (TEM), Raman, Fourier transform infrared (FT-IR) spectroscopy and X-ray photoelectron spectroscopy (XPS). Two kinds of GQDs have been obtained after the treatment of GO with different concentrations of nitric acid. The sizes of GQDs are small, with diameters of 3.38 nm and 2.03 nm on average, respectively. When excited with 365 nm UV light, the two kinds of GQDs exhibit green and yellow luminescence; the different optical properties can be attributed to the differences in degree of oxidation and nitrogen doping. The result is important for GQDs in synthesizing and optical field.

**Keywords:** graphene quantum dots (GQDs); fluorescence; hydrothermal method; nitrogen doping

## 1. Introduction

Graphene, a unique type of two-dimensional semiconductor with superior electronic, thermal, and mechanical properties and chemical stability, has been applied in diverse fields such as electronics, magnetics, and optics [1–4]. Graphene quantum dots (GQDs), a new kind of luminescent zero-dimensional carbon materials with finite size, have attracted tremendous interest from scientists. Because of the quantum confinement in GQDs, it is expected that they will yield many interesting phenomena which do not exist in other semiconductor materials [5,6]. Compared with traditional QDs, GQDs show many advantages, e.g., low toxicity, low-cost synthesizing strategies, good solubility in water, and organic solvents [7]. Therefore, GQDs are considered as promising candidates to replace traditional QDs, and have been integrated into many fields such as bioimaging [8,9], sensing [10], catalysts [11–13], and photovoltaic devices [14].

Nowadays, many methods have been developed to prepare GQDs using large graphene sheets as raw materials through physical and chemical methods, such as hydrothermal and solvothermal treatments, ultrasonic shearing, electrochemical oxidation, and oxygen plasma treating [15–21]. Pan et al. [15,16] synthesized strong blue and green luminescent GQDs by cutting graphene sheets through the hydrothermal route. Concentrated  $H_2SO_4$  and  $HNO_3$  were used to oxidize the graphene sheets. Zhou et al. [17] obtained GQDs by photo-Fenton reaction of graphene oxide (GO) under the UV irradiation, the GQDs have uniform crystallinity, and present a strong photoluminescence property. Li et al. [19] reported an electrochemical approach with a filtration-formed graphene film as a working electrode in PBS for direct preparation of functional GQDs, which exhibited green luminescence. Roy et al. [22] prepared GQDs from plant leaves through a green one-pot hydrothermal

method; GO formed after 2 h and GQDs formed after 8 h of the hydrothermal reaction. The obtained GQDs displayed intense green photoluminescence (PL). Our previous work successfully synthesized different colored GQDs by cutting oxidized GO through a hydrothermal method; the oxidized GO was obtained by oxidation of GO with O<sub>3</sub> [23]. Oxidation is an important part in synthesizing GQDs using graphene, GO, and CNT as starting materials, because it can introduce oxygen-containing groups or defects onto the surface or edge of the carbon materials, and increase active sites. Generally, oxidants used in oxidation include H<sub>2</sub>SO<sub>4</sub>-KMnO<sub>4</sub>, concentrated H<sub>2</sub>SO<sub>4</sub> and HNO<sub>3</sub>, Fenton reagent, O<sub>3</sub>, and so on [15,17,24–26].

Some of the techniques mentioned above are complex and expensive. Dong et.al. [27] prepared single-layered GQDs using SWCNT as a precursor through a simple and green, three-step hydrothermal etching method. They chose different concentrations of HNO<sub>3</sub> as oxidant; the as-prepared GQDs present green and yellow luminescence. Concentrated HNO<sub>3</sub> is excellent in oxidation, introducing nitrogen (N) and oxygen-containing groups into GQDs.

GO, with oxygen-containing groups on the surface and edge has similar sp<sup>2</sup> carbon networks to SWCNT, while it has a layered structure; therefore, it is predicted that GO should be an ideal raw material for preparing GQDs, adopting concentrated HNO<sub>3</sub> as oxidant. However, to the best of our knowledge, no attention has been paid to cutting GO into GQDs by using HNO<sub>3</sub> as oxidant.

In this work, we present a simple, three-step hydrothermal method to synthesize fluorescent GQDs by using GO as raw material and HNO<sub>3</sub> as the oxidant. Two kinds of GQDs with different degrees of oxidation and N doping have been obtained. The mechanism for the formation of GQDs and their fluorescence properties have been discussed in detail.

## 2. Materials and Methods

### 2.1. Materials

All chemicals were analytically pure and used as received. Graphite powder (spectral pure, >99.85%) was purchased from Huayi Company in Shanghai, China, concentrated nitric acid (AR, 65–68%) Guanghua Sci.-Tech Co., Ltd. (Guangzhou, China). Graphene oxide sheets were synthesized with a modified Hummers' method. The water used throughout the experiments was freshly deionized by an ultrapure water system.

### 2.2. Equipments

Scanning electronic microscopy (SEM) images were obtained with a Field-emission scanning electron microscope (S-4800, Hitachi, Tokyo, Japan). High resolution transmission electron microscopic (HR-TEM) images were taken by a TECNAL G2 F20 (FEI Company, Hillsboro, OR, USA) electron microscope operating at 200 kV. Fourier transform infrared (FT-IR) spectra were obtained on a FT-IR spectrometer (NICOLET-6700, Thermo Scientific, Waltham, USA). Raman spectra were recorded on a Lab RAM HR with a 785 nm wavelength laser beam (HORIBA Jobin Yvon S.A.S., Les Ulis, France). X-ray photoelectron spectroscopy (XPS) data were measured by XSAM800 (Kratos, Manchester, UK) with an Al source for determining the composition and chemical bonding configurations. Fluorescence spectra were measured with a F-7000 spectrometer (Hitachi, Tokyo, Japan), which was operated with photomultiplier tube (PMT) voltage at 700 V, slit widths for excitation and emission 2.5 nm and 5.0 nm, respectively.

### 2.3. Synthesis of graphene quantum dots (GQDs)

We prepared GO from graphite adopting a modified Hummers' method [28,29]. The obtained GO was used as the precursor synthesizing GQDs through a three-step, top-down method. Firstly, the proper amount of GO was refluxed with 8 M HNO<sub>3</sub> at 100 °C for 24 h. During the reaction, the color of solvent darkened. When the reaction was complete, the suspension was centrifuged at 2770 g for 10 min after being cooled to room temperature in order to remove the supernatant. The

deposit (labelled as oxidized graphene oxide, O-GO) was collected after being thoroughly washed with deionized (DI) water and centrifuged. Secondly, the obtained O-GO was dispersed in 20 mL DI water, and then heated hydrothermally in a Teflon-lined stainless steel autoclave at 200 °C for 8 h. After that, the obtained suspension was centrifuged with the force of 2770 g for 10 min; a light brown supernatant and black deposit (labelled as reduced O-GO, R-O-GO) was collected. The supernatant showed green fluorescence under 365 nm UV light irradiation, indicating that GQDs were obtained in this procedure [27]. The supernatant was dialyzed over DI water in a dialysis bag with a retained molecular weight of 3500 Da for two weeks, in order to remove acid and impurity ions; the obtained solution was labelled as GQD1. The black sediment was collected, as numerous graphene nanosheets still existed in it. Therefore, the sediment was further refluxed with 15 M HNO<sub>3</sub> at 100 °C for 12 h; after the reaction, the color of solution changed to transparent brown. The strong yellow fluorescence under 365 nm UV light irradiation suggested that a lot of GQDs were released into the solution. After cooling to room temperature, the solution was dialyzed over DI water to remove acid and impurity ions; as a result, GQD2 were collected.

### 3. Results and Discussion

#### 3.1. Characterization and Formation Mechanism of GQDs

Oxidation and hydrothermal treatment modified the structure of GO. Different characterizations were performed to explain the formation mechanism of GQDs. Figure 1 shows the surface morphologies of GO, O-GO, and R-O-GO. Dried GO, O-GO, and R-O-GO exist in sheets, and O-GO and R-O-GO both present metallic appearance. The SEM images show that there are wrinkles at the surface of GO, O-GO and R-O-GO (Figure 2). HR-TEM images (Figure 3) show that GQD1 and GQD2 are nanosheets with small size and circular shape. GQD1 are distributed with diameters ranging from 2.25 to 5.03 nm (3.38 nm in average) and GQD2 1.20 nm to 2.98 nm (2.03 nm on average).

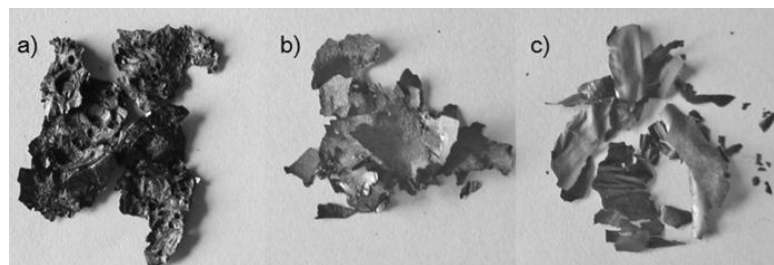


**Figure 1.** Photographs of (a) GO, (b) O-GO and (c) R-O-GO taken under visible light. GO: graphene oxide; O-GO: oxidized graphene oxide; R-O-GO: reduced O-GO.

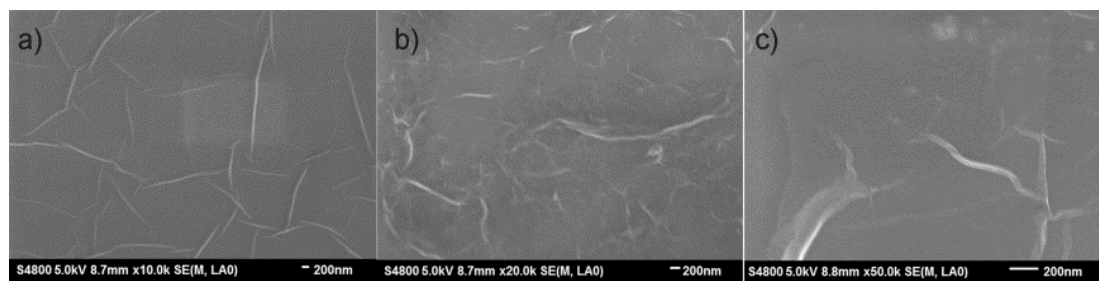


**Figure 2.** Scanning electronic microscopy (SEM) images of (a) GO, (b) O-GO, (c) R-O-GO dispersed in water.

FT-IR analysis of GO, O-GO, and R-O-GO (Figure 4) shows that there are four characteristic peaks at ~3430, ~2360, ~1630, and ~1070 cm<sup>-1</sup>, corresponding to -OH, C=O, C=C, and C-O-C

groups, respectively [30]. The absorption intensity of -OH ( $3437\text{ cm}^{-1}$ ) and C-O-C ( $1070\text{ cm}^{-1}$ ) groups weakens in R-O-GO, suggesting that -OH and C-O-C groups disappear gradually during the hydrothermal treatment.

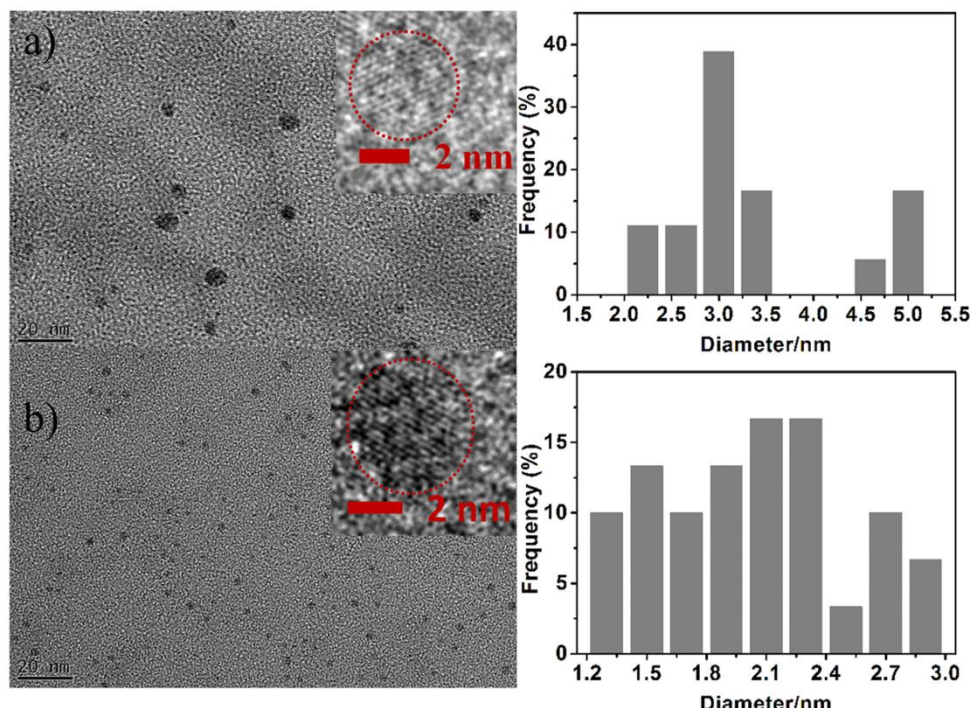


**Figure 3.** High resolution transmission electron microscopy (HR-TEM) images of (a) GQD1 and (b) GQD2. The insets in (a,b) are the corresponding representative images of individual GQD1 and GQD2. The right column shows the diameter distribution of GQD1 and GQD2.

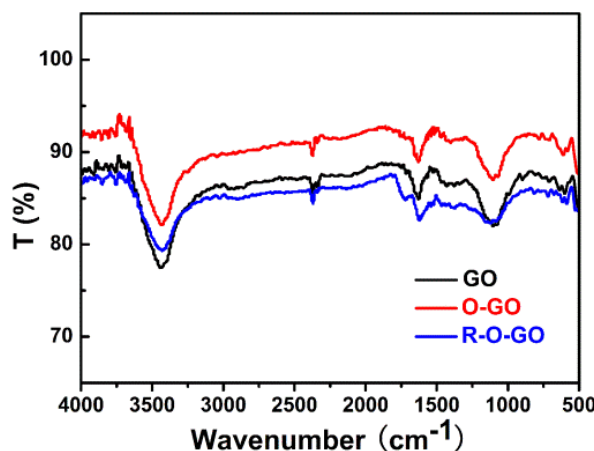


**Figure 4.** Fourier transform infrared (FT-IR) spectra of GO, O-GO and R-O-GO.

Furthermore, chemical oxidation can create a lot of disordered structures in GO, which is revealed by the Raman spectra (Figure 5). The G band is associated with  $E_{2g}$  vibrational modes of the  $\text{sp}^2$  carbon atom, and the D band represents the edge defect and amorphous graphitic system [31,32]. The intensity ratio  $I_D/I_G$ , “disorder structure” to the “crystalline structure” is adopted to evaluate the structure of different oxidized GO. An increase in the  $I_D/I_G$  means an increase in the amount of topological disorder in the graphite layer and a decrease in the size of nanocrystalline graphite [30]. The Raman Spectra of GO, O-GO and R-O-GO given in Figure 5 show that the D and G bands are

1345 and  $1588\text{ cm}^{-1}$ , respectively. The intensity ratio  $I_D/I_G$  decreases from 1.02 (GO) to 0.96 (O-GO), which is contrary to the general rule. We deduce that after the treatment of GO by  $\text{HNO}_3$ , the obtained O-GO is of relatively high quality. However, the O-GO exhibits a broader D band, which indicates that the intercalation of N atoms and oxygen-containing groups leads to somewhat disordered structures. This result is similar to a previously-reported conclusion [20]. It was predicted that the intensity ratio  $I_D/I_G$  of GO would significantly decrease after reduction as the  $\text{sp}^2$  structure restored. However, the  $I_D/I_G$  was found to be 1.15 in R-O-GO after hydrothermal treatment, which is larger than that in O-GO. Similar results have also been reported elsewhere in the literature [33,34]. We deduce that the increase of the  $I_D/I_G$  ratio after chemical reduction can be attributed to the decrease in the average size of the  $\text{sp}^2$  domains upon reduction of O-GO, in which newly-created graphitic domains are more numerous in number, but smaller in size, than those present in O-GO. Besides that, the increased fraction of graphene edges could also contribute to the increase in the  $I_D/I_G$  ratio, which is in accordance with the reported results [33,35].

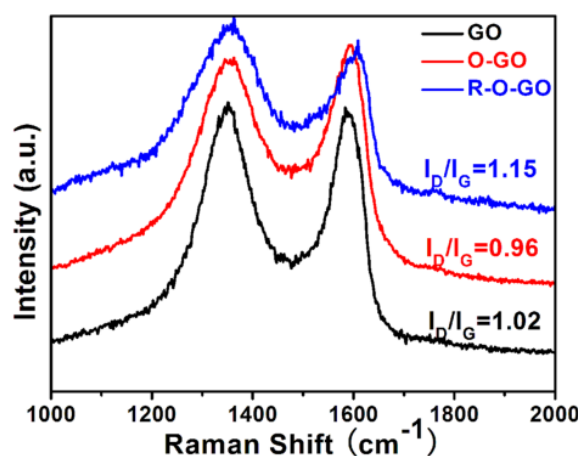


**Figure 5.** Raman spectra of GO, O-GO and R-O-GO.

The chemical structure and the type of oxygen-containing groups of GO changed after oxidation and hydrothermal treatment. XPS analysis indicates that N atoms are introduced into GO after oxidation by  $\text{HNO}_3$ , as shown in Figure 6. The high-resolution XPS spectra of C 1s further confirm the chemical structure change during the oxidation and hydrothermal treatment. As shown in Figure 7, different types of C atoms exist, including C-C/C=C ( $\sim 284.5\text{ eV}$ ), C-N ( $\sim 285.6\text{ eV}$ ), C-O-C/C-OH ( $\sim 286.5\text{ eV}$ ) and C=O/COOH ( $\sim 287.8\text{ eV}$ ) [30,36]. There are mainly carboxyl and epoxy groups in GO prepared by Hummers' method, the amount of C-O increases while C-C and C=C decreases after oxidation by  $\text{HNO}_3$ , which indicates that oxidation makes the C-C and C=C bonds break and attach to oxygen-containing groups. The amount of C increases and O decreases in R-O-GO, which can be explained from the fact that a lot of oxygen-containing groups are released in the form of  $\text{CO}_2$ , CO, and  $\text{H}_2\text{O}$  during the hydrothermal treatment [23]. The decreased amount of C-O-C and C-O in R-O-GO is in good agreement with the results of FT-IR. Moreover, the high-resolution XPS spectra of N 1s (Figure 8a,b) also show that C-N exists in O-GO and R-O-GO, suggesting that N atoms are introduced into GO in different forms including C-N-C ( $\sim 399.5\text{ eV}$ ) and N-(C)<sub>3</sub> ( $\sim 401.5\text{ eV}$ ) [37–39]. The XPS results indicate that both GQD1 and GQD2 are composed of carbon, oxygen, hydrogen, and nitrogen (Figures 7 and 8). N 1s analysis shows that N exists in GQD1 in the forms of C-N-C and N-(C)<sub>3</sub>, while in GQD2, besides the two forms of N, -NO<sub>2</sub> (406.4 eV) also exists [37,39–42]; see in Figure 8c,d. XPS analysis gives more information about the chemical structure of the studied systems. Element analysis of GO, O-GO and R-O-GO by FT-IR and XPS presents similar results; these techniques are complementary and exhibit more accurate conclusions when used together.

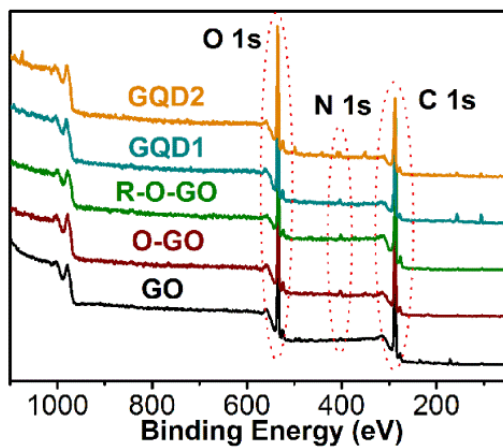


**Figure 6.** XPS survey of GO, O-GO, R-O-GO, GQD1 and GQD2.

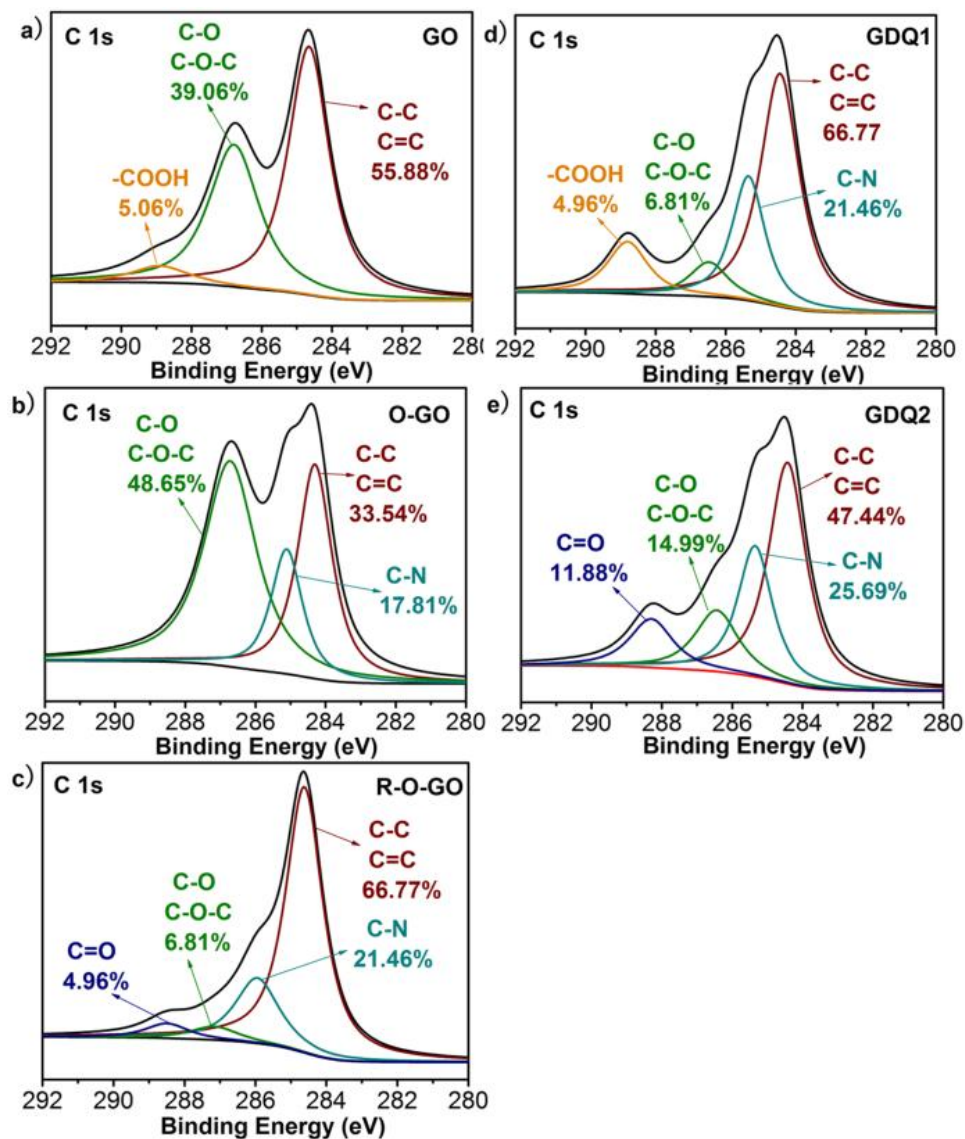


**Figure 7.** High resolution XPS spectra of C 1s for (a) GO, (b) O-GO, (c) R-O-GO, (d) GQD1 and (e) GQD2.

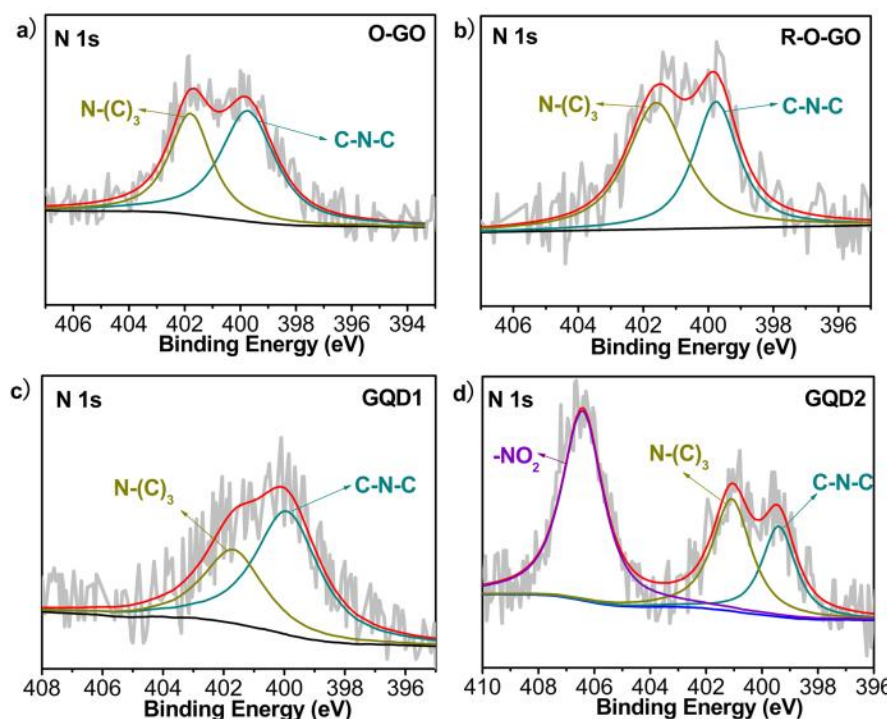


**Figure 8.** High resolution XPS spectra of N 1s for (a) O-GO, (b) R-O-GO, (c) GQD1 and (d) GQD2.

Based on the results mentioned above, a possible mechanism for the formation of the GQDs can be proposed. GO was initially oxidized to O-GO during the chemical oxidation with 8 M HNO<sub>3</sub>, producing a lot of oxygen-containing groups and introducing N atoms. After that, the structure of O-GO was decomposed, because the oxygen-containing groups were partially removed, forming a lot of nanosheets (R-O-GO) by the hydrothermal method under the continuous high-temperature and high-pressure conditions. Meanwhile, plenty of graphene quantum dots (GQD1) were formed and released into the solution. Finally, the collected R-O-GO was further oxidized with concentrated HNO<sub>3</sub>. Chemical oxidation is an effective method to release GQDs from their aggregates into solution [43]. As a result, a lot of GQD2 were released into the solution after R-O-GO was refluxed with 15 M HNO<sub>3</sub> for 12 h.

### 3.2. Fluorescence Properties of GQDs

The aqueous solutions of GQD1 and GQD2 are light brown under visible light, but they have different fluorescence under an excitation of a beam of 365 nm. GQD1 and GQD2 exhibit green and yellow fluorescence, respectively. Figure 9 demonstrates the PL spectra of the two GQDs. The emission spectra of GQD1 show obvious excitation-dependence. With the gradual increase of the excitation wavelength from 280 nm to 480 nm, the maximum emission wavelength of GQD1 is red-shifted from 408 nm to 500 nm. However, the emission wavelength of GQD2 keeps stable at about 535 nm during the excitation wavelengths we employed. The different PL properties of GQD1 and GQD2 may be attributed to their size and surface state, which are affected by functional groups [7,36,44,45]. Surface decoration degree and size can change the energy gap of GQD, thus affecting the PL properties. Our analysis of HR-TEM shows that GQD1 are larger than GQD2 in size; this can lead to a red shift of GQD1 compared to GQD2, which is contrary to our result. Therefore, surface decoration is the major reason for the different PL properties. XPS analysis shows that N and O atoms exist in both GQD1 and GQD2; C 1s XPS indicates that the amounts of N and O are greater in GQD2 than GQD1 (Figure 7d,e). In addition, N atoms doped in GQDs with different forms: besides C-N-C and N-(C)<sub>3</sub>, -NO<sub>2</sub> can be found in GQD2 (Figure 8c,d). From the above analysis, it is reasonable to conclude that the difference

in optical properties between GQD1 and GQD2 should be attributed to their differences in degree of oxidation and N doping.

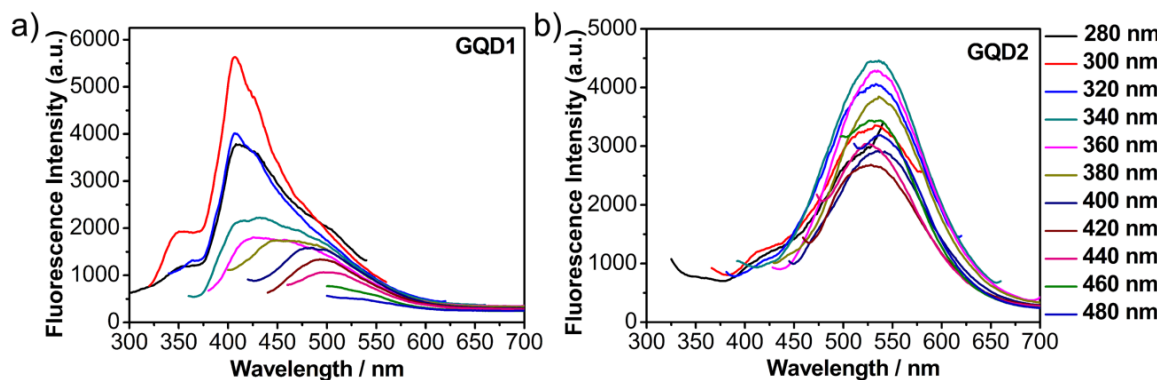


**Figure 9.** Fluorescence spectra of (a) GQD1 and (b) GQD2 under different excitation wavelengths.

#### 4. Conclusions

A simple three-step method to prepare small-sized GQDs, adopting GO as precursor, has been developed. In the first step, GO was oxidized into O-GO by 8 M HNO<sub>3</sub>. Secondly, the obtained O-GO was dispersed in DI water and heated hydrothermally to 200 °C, resulting in the formation of GQD1 and R-O-GO. Finally, R-O-GO was refluxed with 15 M HNO<sub>3</sub> under 100 °C, forming GQD2. The diameters of GQD1 and GQD2 are 3.38 nm and 2.03 nm on average, respectively. Oxidation by HNO<sub>3</sub> results in the introduction of N atoms and oxygen-containing groups. N atoms doped in GQDs in the form of C-N-C and N-(C)<sub>3</sub> and -NO<sub>2</sub>. The GQDs show different optical properties, which is caused by the different degree of oxidation and N doping.

**Author Contributions:** Meilian Zhao conceived, designed, performed the experiments and wrote the paper.

**Funding:** This research was funded by the National Natural Science Foundation of China (81503366) and Natural Science Foundation of the Education Department of Sichuan Province (16ZA0109).

**Acknowledgments:** We sincerely thank Prof. Yong Guo and Dan Xiao and Dr. Feng Yang in College of Chemistry, Sichuan University for providing important suggestions and help in this work.

**Conflicts of Interest:** The author declares no conflict of interest.

#### References

- Novoselov, K.S.; Geim, A.K.; Morozov, S.V.; Jiang, D.; Zhang, Y.; Dubonos, S.V.; Grigorieva, I.V.; Firsov, A.A. Electric field effect in atomically thin carbon films. *Science* **2004**, *306*, 666–669. [[CrossRef](#)] [[PubMed](#)]
- Kuila, T.; Mishra, A.K.; Khanra, P.; Kim, N.H.; Lee, J.H. Recent advances in the efficient reduction of graphene oxide and its application as energy storage electrode materials. *Nanoscale* **2013**, *5*, 52–71. [[CrossRef](#)] [[PubMed](#)]
- Shen, F.; Wang, D.; Liu, R.; Pei, X.; Zhang, T.; Jin, J. Edge-tailored graphene oxide nanosheet-based field effect transistors for fast and reversible electronic detection of sulfur dioxide. *Nanoscale* **2013**, *5*, 537–540. [[CrossRef](#)] [[PubMed](#)]
- Fowler, J.D.; Allen, M.J.; Tung, V.C.; Yang, Y.; Kaner, R.B.; Weiller, B.H. Practical chemical sensors from chemically derived graphene. *ACS Nano* **2009**, *3*, 301–306. [[CrossRef](#)] [[PubMed](#)]
- Son, Y.W.; Cohen, M.L.; Louie, S.G. Energy gaps in graphene nanoribbons. *Phys. Rev. Lett.* **2006**, *97*, 216803. [[CrossRef](#)] [[PubMed](#)]
- Nakada, K.; Fujita, M.; Dresselhaus, G.; Dresselhaus, M.S. Edge state in graphene ribbons: Nanometer size effect and edge shape dependence. *Phys. Rev. B* **1996**, *54*, 17954–17961. [[CrossRef](#)]
- Shen, J.; Zhu, Y.; Yang, X.; Li, C. Graphene quantum dots: emergent nanolights for bioimaging, sensors, catalysis and photovoltaic devices. *Chem. Commun.* **2012**, *48*, 3686–3699. [[CrossRef](#)] [[PubMed](#)]

8. Liu, Q.; Guo, B.; Rao, Z.; Zhang, B.; Gong, J.R. Strong two-photon-induced fluorescence from photostable, biocompatible nitrogen-doped graphene quantum dots for cellular and deep-tissue imaging. *Nano Lett.* **2013**, *13*, 2436–2441. [[CrossRef](#)] [[PubMed](#)]
9. Lv, O.Y.; Tao, Y.X.; Qin, Y.; Chen, C.X.; Pan, Y.; Deng, L.H.; Liu, L.; Kong, Y. Highly fluorescent and morphology-controllable graphene quantum dots-chitosan hybrid xerogels for in vivo imaging and pH-sensitive drug carrier. *Mater. Sci. Eng. C* **2016**, *67*, 478–485. [[CrossRef](#)] [[PubMed](#)]
10. Tan, F.; Cong, L.; Li, X.; Zhao, Q.; Zhao, H.; Quan, X.; Chen, J. An electrochemical sensor based on molecularly imprinted polypyrrole/graphene quantum dots composite for detection of bisphenol A in water samples. *Sens. Actuat. B-Chem* **2016**, *233*, 599–606. [[CrossRef](#)]
11. Liu, K.; Song, Y.; Chen, S. Oxygen reduction catalyzed by nanocomposites based on graphene quantum dots-supported copper nanoparticles. *Int. J. Hydrogen Energy* **2016**, *41*, 1559–1567. [[CrossRef](#)]
12. Tian, H.W.; Shen, K.; Hu, X.Y.; Qiao, L.; Zheng, W.T. N, S co-doped graphene quantum dots-graphene-TiO<sub>2</sub> nanotubes composite with enhanced photocatalytic activity. *J. Alloy. Compd.* **2017**, *691*, 369–377. [[CrossRef](#)]
13. Shen, K.; Xue, X.; Wang, X.Y.; Hu, X.Y.; Tian, H.W.; Zheng, W.T. One-step synthesis band-tunable N, S co-doped commercial TiO<sub>2</sub>/graphene quantum dots composite with enhanced photocatalytic activity. *RSC Adv.* **2017**, *7*, 23319–23327. [[CrossRef](#)]
14. Moon, B.J.; Lee, K.S.; Shim, J.; Park, S.; Kim, S.H.; Bae, S.; Park, M.; Lee, C.L.; Choi, W.K.; Yi, Y.; et al. Enhanced photovoltaic performance of inverted polymer solar cells utilizing versatile chemically functionalized ZnO@graphene quantum dot monolayer. *Nano Energy* **2016**, *20*, 221–232. [[CrossRef](#)]
15. Pan, D.Y.; Zhang, J.C.; Li, Z.; Wu, M.H. Hydrothermal route for cutting graphene sheets into blue-luminescent graphene quantum dots. *Adv. Mater.* **2010**, *22*, 734–738. [[CrossRef](#)] [[PubMed](#)]
16. Pan, D.Y.; Guo, L.; Zhang, J.C.; Xi, C.; Xue, Q.; Huang, H.; Li, J.H.; Zhang, Z.W.; Yu, W.J.; Chen, Z.W.; et al. Cutting sp(2) clusters in graphene sheets into colloidal graphene quantum dots with strong green fluorescence. *J. Mater. Chem.* **2012**, *22*, 3314–3318. [[CrossRef](#)]
17. Zhou, X.; Zhang, Y.; Wang, C.; Wu, X.; Yang, Y.; Zheng, B.; Wu, H.; Guo, S.; Zhang, J. Photo-fenton reaction of graphene oxide: a new strategy to prepare graphene quantum dots for DNA cleavage. *ACS Nano* **2012**, *6*, 6592–6599. [[CrossRef](#)] [[PubMed](#)]
18. Zhuo, S.; Shao, M.; Lee, S.T. Upconversion and downconversion fluorescent graphene quantum dots: ultrasonic preparation and photocatalysis. *ACS Nano* **2012**, *6*, 1059–1064. [[CrossRef](#)] [[PubMed](#)]
19. Li, Y.; Hu, Y.; Zhao, Y.; Shi, G.Q.; Deng, L.E.; Hou, Y.B.; Qu, L.T. An electrochemical avenue to green-luminescent graphene quantum dots as potential electron-acceptors for photovoltaics. *Adv. Mater.* **2011**, *23*, 776–780. [[CrossRef](#)] [[PubMed](#)]
20. Li, Y.; Zhao, Y.; Cheng, H.; Hu, Y.; Shi, G.; Dai, L.; Qu, L. Nitrogen-doped graphene quantum dots with oxygen-rich functional groups. *J. Am. Chem. Soc.* **2012**, *134*, 15–18. [[CrossRef](#)] [[PubMed](#)]
21. Gokus, T.; Nair, R.R.; Bonetti, A.; Boehmle, M.; Lombardo, A.; Novoselov, K.S.; Geim, A.K.; Ferrari, A.C.; Hartschuh, A. Making graphene luminescent by oxygen plasma treatment. *ACS Nano* **2009**, *3*, 3963–3968. [[CrossRef](#)] [[PubMed](#)]
22. Roy, P.; Periasamy, A.P.; Chuang, C.; Liou, Y.R.; Chen, Y.F.; Joly, J.; Liang, C.T.; Chang, H.T. Plant leaf-derived graphene quantum dots and applications for white LEDs. *New J. Chem.* **2014**, *38*, 4946–4951. [[CrossRef](#)]
23. Yang, F.; Zhao, M.L.; Zheng, B.Z.; Xiao, D.; Wu, L.; Guo, Y. Influence of pH on the fluorescence properties of graphene quantum dots using ozonation pre-oxide hydrothermal synthesis. *J. Mater. Chem.* **2012**, *22*, 25471–25479. [[CrossRef](#)]
24. Galande, C.; Mohite, A.D.; Naumov, A.V.; Gao, W.; Ci, L.J.; Ajayan, A.; Gao, H.; Srivastava, A.; Weisman, R.B.; Ajayan, P.M. Quasi-molecular fluorescence from graphene oxide. *Sci. Rep.* **2011**, *1*, 1–5. [[CrossRef](#)] [[PubMed](#)]
25. Chen, J.L.; Yan, X.P.; Meng, K.; Wang, S.F. Graphene oxide based photoinduced charge transfer label-free near-infrared fluorescent biosensor for dopamine. *Anal. Chem.* **2011**, *83*, 8787–8793. [[CrossRef](#)] [[PubMed](#)]
26. Liu, L.V.; Tian, W.Q.; Wang, Y.A. Ozonization at the vacancy defect site of the single-walled carbon nanotube. *J. Phys. Chem. B* **2006**, *110*, 13037–13044. [[CrossRef](#)] [[PubMed](#)]
27. Dong, Y.; Pang, H.; Ren, S.; Chen, C.; Chi, Y.; Yu, T. Etching single-wall carbon nanotubes into green and yellow single-layer graphene quantum dots. *Carbon* **2013**, *64*, 245–251. [[CrossRef](#)]
28. Xu, Y.X.; Bai, H.; Lu, G.W.; Li, C.; Shi, G.Q. Flexible graphene films via the filtration of water-soluble noncovalent functionalized graphene sheets. *J. Am. Chem. Soc.* **2008**, *130*, 5856–5857. [[CrossRef](#)] [[PubMed](#)]

29. Kovtyukhova, N.I.; Ollivier, P.J.; Martin, B.R.; Mallouk, T.E.; Chizik, S.A.; Buzaneva, E.V.; Gorchinskiy, A.D. Layer-by-layer assembly of ultrathin composite films from micron-sized graphite oxide sheets and polycations. *Chem. Mater.* **1999**, *11*, 771–778. [[CrossRef](#)]
30. Lin, Z.; Yao, Y.; Li, Z.; Liu, Y.; Li, Z.; Wong, C.P. Solvent-assisted thermal reduction of graphite oxide. *J. Phys. Chem. C* **2010**, *114*, 14819–14825. [[CrossRef](#)]
31. Casiraghi, C.; Hartschuh, A.; Qian, H.; Piscanec, S.; Georgi, C.; Fasoli, A.; Novoselov, K.S.; Basko, D.M.; Ferrari, A.C. Raman spectroscopy of graphene edges. *Nano Lett.* **2009**, *9*, 1433–1441. [[CrossRef](#)] [[PubMed](#)]
32. Malard, L.M.; Pimenta, M.A.; Dresselhaus, G.; Dresselhaus, M.S. Raman spectroscopy in graphene. *Phys. Rep.* **2009**, *473*, 51–87. [[CrossRef](#)]
33. Ren, P.G.; Yan, D.X.; Ji, X.; Chen, T.; Li, Z.M. Temperature dependence of graphene oxide reduced by hydrazine hydrate. *Nanotechnology* **2011**, *22*, 055705. [[CrossRef](#)] [[PubMed](#)]
34. Qian, M.; Feng, T.; Ding, H.; Lin, L.; Li, H.; Chen, Y.; Sun, Z. Electron field emission from screen-printed graphene films. *Nanotechnology* **2009**, *20*, 425702. [[CrossRef](#)] [[PubMed](#)]
35. Bo, Z.; Shuai, X.; Mao, S.; Yang, H.; Qian, J.; Chen, J.; Yan, J.; Cen, K. Green preparation of reduced graphene oxide for sensing and energy storage applications. *Sci. Rep.* **2014**, *4*, 4684. [[CrossRef](#)] [[PubMed](#)]
36. Li, L.L.; Ji, J.; Fei, R.; Wang, C.Z.; Lu, Q.; Zhang, J.R.; Jiang, L.P.; Zhu, J.J. A facile microwave avenue to electrochemiluminescent two-color graphene quantum dots. *Adv. Funct. Mater.* **2012**, *22*, 2971–2979. [[CrossRef](#)]
37. Lu, W.; Qin, X.; Liu, S.; Chang, G.; Zhang, Y.; Luo, Y.; Asiri, A.M.; Al-Youbi, A.O.; Sun, X. Economical, green synthesis of fluorescent carbon nanoparticles and their use as probes for sensitive and selective detection of mercury (II) ions. *Anal. Chem.* **2012**, *84*, 5351–5357. [[CrossRef](#)] [[PubMed](#)]
38. Wang, Y.; Shao, Y.; Matson, D.W.; Li, J.; Lin, Y. Nitrogen-doped graphene and its application in electrochemical biosensing. *ACS Nano* **2010**, *4*, 1790–1798. [[CrossRef](#)] [[PubMed](#)]
39. Shao, Y.; Zhang, S.; Engelhard, M.H.; Li, G.; Shao, G.; Wang, Y.; Liu, J.; Aksay, I.A.; Lin, Y. Nitrogen-doped graphene and its electrochemical applications. *J. Mater. Chem.* **2010**, *20*, 7491–7496. [[CrossRef](#)]
40. Matter, P.H.; Zhang, L.; Ozkan, U.S. The role of nanostructure in nitrogen-containing carbon catalysts for the oxygen reduction reaction. *J. Catal.* **2006**, *239*, 83–96. [[CrossRef](#)]
41. Arrigo, R.; Haevecker, M.; Schloegl, R.; Su, D.S. Dynamic surface rearrangement and thermal stability of nitrogen functional groups on carbon nanotubes. *Chem. Commun.* **2008**, 4891–4893. [[CrossRef](#)] [[PubMed](#)]
42. Yang, F.; Zhao, M.L.; Ji, H.Y.; He, D.H.; Wu, L.; Zheng, B.Z.; Xiao, D.; Guo, Y. Solvothermal synthesis of oxygen/nitrogen functionalized graphene-like materials with diversified morphology from different carbon sources and their fluorescence properties. *J. Mater. Sci.* **2015**, *50*, 1300–1308. [[CrossRef](#)]
43. Liu, R.; Wu, D.; Feng, X.; Müllen, K. Bottom-up fabrication of photoluminescent graphene quantum dots with uniform morphology. *J. Am. Chem. Soc.* **2011**, *133*, 15221–15223. [[CrossRef](#)] [[PubMed](#)]
44. Zhu, S.; Zhang, J.; Tang, S.; Qiao, C.; Wang, L.; Wang, H.; Liu, X.; Li, B.; Li, Y.; Yu, W. Surface chemistry routes to modulate the photoluminescence of graphene quantum dots: From fluorescence mechanism to up-conversion bioimaging applications. *Adv. Funct. Mater.* **2012**, *22*, 4732–4740. [[CrossRef](#)]
45. Bao, L.; Zhang, Z.L.; Tian, Z.Q.; Zhang, L.; Liu, C.; Lin, Y.; Qi, B.; Pang, D.W. Electrochemical tuning of luminescent carbon nanodots: From preparation to luminescence mechanism. *Adv. Mater.* **2011**, *23*, 5801–5806. [[CrossRef](#)] [[PubMed](#)]



© 2018 by the author. Licensee MDPI, Basel, Switzerland. This article is an open access article distributed under the terms and conditions of the Creative Commons Attribution (CC BY) license (<http://creativecommons.org/licenses/by/4.0/>).